

Hormigón 3D estructural y su aplicación en Tor Alva, la torre más alta del mundo impresa en 3D

Fully load-bearing reinforced 3D printed concrete and its application in Tor Alva, the world-tallest 3D printed concrete tower

Alejandro Giraldo Soto^a, Ana Anton^b, Lukas Gebhard^c, Jürg Conzett^d,
Walter Kaufmann^e, Benjamin Dillenburger^f and Michael Hansmeyer^g

^a Doctor, Ingeniero de Caminos, Canales y Puertos. ETH Zurich. Senior Researcher. giraldo@ibk.baug.ethz.ch

^b Architect. ETH Zurich. Postdoctoral Researcher. anton@arch.ethz.ch

^c Dr. Sc. ETH, Civil Engineer ETH/SIA. ETH Zurich. Postdoctoral Researcher. gebhard@ibk.baug.ethz.ch

^d Civil Engineer ETH/SIA. Conzett Bronzini Partner AG. Senior Partner. j.conzett@cbp.ch

^e Doctor, Ingeniero de Caminos, Canales y Puertos. ETH Zurich. Full Professor. kaufmann@ibk.baug.ethz.ch

^f Architect. ETH Zurich. Full Professor. dillenburger@arch.ethz.ch

^g Architect. ETH Zurich. Computational Architecture. hansmeyer@arch.ethz.ch

RESUMEN

El hormigón 3D (H3D) es un novedoso método de construcción que avanza rápidamente y que aún no está recogido por las normas actuales al carecer de modelos mecánicos, conceptos de armado y de validaciones estructurales en realizaciones a escala real. Tor Alva, torre H3D de 30 m de altura y la más alta de su tipología, es este tipo de realización a escala real construida en los Alpes suizos (2024-2025). Este artículo presenta (i) la descripción general y el concepto estructural de Tor Alva y (ii) los resultados experimentales de los ensayos a escala 1:1 de las V-columnas H3D reforzado de Tor Alva.

ABSTRACT

Digital fabrication with concrete (DFC), particularly 3D printed concrete (3DPC), is a rapidly advancing construction method. However, it is not yet covered by current standards and lacks established mechanical models, reinforcement concepts, and load-bearing validation for full-scale structures. Tor Alva, a 30-meter-high tower and the tallest of its kind, is an example of a full-scale application (2024-2025) in the Swiss Alps using DFC. This paper presents (i) an overview and the structural concept of Tor Alva and (ii) the experimental results of full-scale tests on the reinforced 3DPC V-columns of Tor Alva.

PALABRAS CLAVE: Hormigón 3D estructural, concreto 3D, ensayos hormigón 3D, construcción H3D.

KEYWORDS: Digital Fabrication, reinforced 3DPC, full-scale 3DPC testing, 3DPC construction.

1. Introduction

The construction industry seeks new materials and methods to enhance building flexibility, sustainability and efficiency. Digital fabrication with concrete (DFC), especially through 3D printed concrete (3DPC), is rapidly advancing and has seen significant growth in

construction applications in recent years. While this technology promises increasing sustainability and efficiency, progress in sustainability has been limited [1]. This shortfall is attributed to (i) the predominant use of 3DPC for elements with low structural demand

(comparable to masonry) rather than actually substituting structural concrete and (ii) the absence of a well-defined design basis for load-bearing 3DPC [2]. Advancing load-bearing applications has the potential to drive significant impact, as the technology enables the production of more efficient structures with substantially lower material consumption. However, the implementation of load-bearing reinforced 3DPC for elements with high structural demand is progressing slowly, with no known full-scale construction projects completed to date. As a result, full-scale structural projects are crucial for evaluating the sustainability and efficiency of DFC. 3D printed concrete has non-isotropic properties caused by the 3D printed concrete layers that differ from conventional cast concrete. Despite numerous research efforts at ETH Zurich [2]–[7] and by other researchers worldwide [8]–[11], significant progress is still needed before the design of load-bearing reinforced 3DPC elements is incorporated into standards. Key challenges include the development and validation of concepts for reinforcement integration, mechanical models, and an overall design basis.

Tor Alva is an example of a full-scale project, see Figure 1. It is a 30 m high tower built in the Swiss Alps using DFC with pioneering structural concepts and digital technologies. Its structure consists of a modular system featuring fully load-bearing reinforced 3DPC columns and is currently the world’s tallest structure of its kind. At ETH Zurich, the three Chairs of Concrete Structures and Bridge Design, Digital Building Technologies and Physical Chemistry of Building Materials have jointly carried out research based on experimental campaigns and prototypes in 3DPC to assess the 3DPC performance, develop mechanical models, contribute to building the design basis for 3DPC, validate the concepts of reinforcement integration and conceive the design of Tor Alva by exploiting the load-bearing reinforced 3DPC capabilities.

This paper (i) presents an overview and the structural concept of Tor Alva and (ii) the experimental results of full-scale tests on the load-bearing reinforced 3DPC V-columns of Tor Alva.

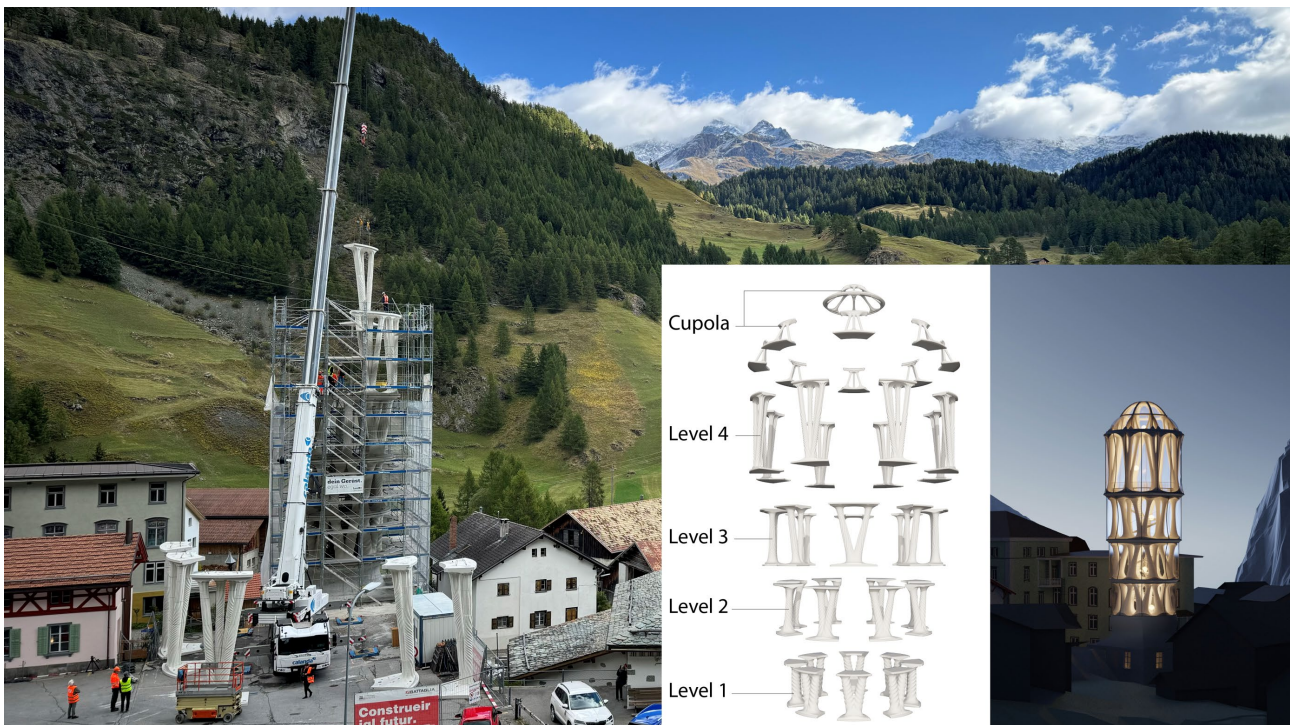


Figure 1. Tor Alva: Assembly of load-bearing 3DPC columns of level 4 (30.09.2024), overview of the column assembly and visualisation.

2. Tor Alva

Construction of the load-bearing structure of Tor Alva, designed to showcase DFC's construction and structural potential, was completed in November 2024. Tor Alva also emphasises circularity, allowing for disassembly and reuse (see the overview of the 3DPC V-column assembly in Figure 1).

Tor Alva was designed and built in collaboration with ETH Zurich, Conzett Bronzini Partners AG and Zindel United AG. With this project the client, Nova Fundaziun Origen, aims to revitalize the mountain village of Mulegns with this project. The tower serves as a landmark for regional tourism, enhancing the architectural and cultural profile of Grisons and Switzerland while promoting knowledge transfer. Tor Alva showcases market-ready innovations in the world's tallest digitally printed building, highlighting the application of structural 3DPC, and the potential for modular, circular, and scalable construction with DFC.

2.1 Boundary conditions

The dimensions of the tower are limited by the adjoining buildings, the urban planning specifications and the existing building on which the tower rests. On this basis, the tower was designed as a cylindrical vertical extension of an existing building with a rectangular footprint measuring 8.5 by 7.5 m². To ensure structural integrity, the existing building was strengthened with a reinforced concrete (RC) frame connecting the tower to the foundations. The transition from the rectangular base to the cylindrical tower is seamlessly achieved through a double-curved RC shell. The organic form of the tower incorporates branching columns placed around a central helical staircase. As Tor Alva was intended to remain in Mulegns for the

short to medium term, it was essential to conceive a modular design that could be easily dismantled, reassembled, and reused elsewhere.

The architectural integration between the existing building and the tower, combined with the desire to enhance the users' experience as they ascend the tower, is evident in the careful design of the spaces and structural elements. The promenade through the tower starts from the old structure that marks the entrance with a closed, defined space. Ascending the four levels of the tower, the columns transform from wide elements with a height of 3.4 meters to slender 6-meter-tall elements. On the fourth floor, visitors reach the main space of the tower, dedicated to the performing arts. This area is defined by eight perimetral columns, each having four branches, covered by a cupola consisting of spatially arranged filigree elements.

2.2 Pioneering and innovations

The tower consists of 32 fully structural thin-shelled concrete columns that have been robotically 3D printed and reinforced. These pioneering reinforced 3DPC V-columns are characterised by several distinctive features, such as: (i) fully load-bearing columns with integrated transverse and longitudinal reinforcement (main innovation), (ii) a segmentation system for 3DCP components eliminating the limitations of the maximum length of a continuous printable element, and (iii) segmental construction system at building scale allowing for disassembly and reuse. It also improves constructability by using more manageable segments that are lighter and have reduced dimensions, making them easier to handle and assemble.

2.3 Construction

The construction process is divided into two stages: (i) prefabrication and (ii) on-site assembly.

2.3.1. Prefabrication of components

This stage of construction focuses on fabricating segments and assembling them into the V-shaped structural elements of the tower. A parallelised production process was employed: the precast base and capital of the column were produced in a factory using conventional construction methods, while 3DPC components were produced separately at ETH Zurich. The segments were transported to the prefabrication hall, located 10 km from the construction site, where the components were assembled as follows: (i) positioning of the precast base; (ii) connection of the 3DPC V-segment of the column to the base by using an epoxy; (iii) attachment of the 3DPC extensions of each branch and gluing with an epoxy; (iv) positioning and connection of the capital; (v) insertion of longitudinal reinforcement into the hollow channels connecting all the components; and (vi) grouting the channels 24 hours after applying the last epoxy layer. The individual segments of one column are visible in Figure 2. After grouting, the monolithic elements were ready to be transported to the construction site, where the modular assembly process took place.

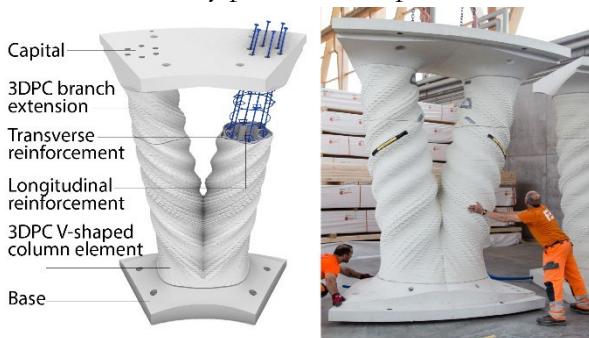


Figure 2. Level 1 column of Tor Alva: Components and prefabricated elements

2.3.2. On-site assembly

On-site assembly of the structural components began after completing all the components of one level. Columns were transported to the construction site by truck and positioned with a crane. The assembly process was highly efficient, taking just one day per level. After positioning the columns, their bases and capitals were

secured with bolts. Next, to ensure proper load transfer, a self-levelling mortar was poured between the capitals and bases of each level. This approach, which is based on modularity and prefabrication, ensures on-site safety and on-time construction.

3. Structural concept of Tor Alva

3.1 Tower concept and boundary conditions

The whole structure of Tor Alva consists of an existing reinforced building and foundations which serve as the base of the tower, a double-curved RC transition shell and the proper 3DPC structure. The latter consists of a modular system featuring fully load-bearing reinforced 3DPC V-columns. It exploits the capabilities of 3DPC by leveraging it as a fully load-bearing material, with integrated transverse and vertical reinforcement resisting to ensure structural integrity just like ordinary RC.

The structural concept of the tower is strongly framed by the requirements imposed by (i) the boundary conditions: base on existing building and circularity allowing disassembly and reuse; (ii) the pioneering and innovative architectural and structural requirements: organic geometries, load-bearing 3DPC and feasible reinforcement integration strategies; (iii) constructability; (iv) functional and structural requirements; and (v) uncertainties associated with the performance of the 3DPC.

There were three design challenges associated to 3DPC structure: one related to finding a structural system that works mainly via normal forces to reduce the uncertainties of the 3DPC column performance subjected to bending moments (tensile forces could be controlled by post-tensioning); second, to define a reinforced 3DPC columns concept with viable strategies that integrate reinforcement and exploit the 3DPC material as a load-bearing element; and third, how to assemble all parts.

As a result of a successful interdisciplinary collaboration, involving several experimental campaigns, a configuration of columns in V- and A-shapes, forming a spatial truss consisting of stiff horizontal rings and diagonal struts was chosen. This system is structurally efficient, as both vertical and horizontal actions generate predominantly axial (tensile and compressive) forces. The structural performance was experimentally validated (see Section 4), showing a good performance of the reinforced 3DPC columns subjected to tensile forces and bending moments. This led to ruling out the post-tensioning of the columns of Levels 1, 2, and 3.

The dimensioning of the 3DPC was performed using conventional calculation methods (FEM models consisting of frame elements), accounting for the 3DPC particularities in sectional design, ensuring a favourable load transfer system and in the detailing. The design compressive and tensile loads N_d of the columns ranged from -320 kN to $+85$ kN. Taking into account the small force eccentricities, the compressive stresses in the 3DPC columns reach -5.4 MPa at the Ultimate Limit State (ULS) with wind as leading variable action. Tensile forces resisted by mild reinforcement, usually 4 to 6 bars $\varnothing 16$ mm per column branch in Levels 1 to 3. The columns of the higher levels are posttensioned by one central high-tension steel bar $\varnothing 12$ mm with an initial force of $P_0 = 124$ kN. These bars are greased and run-in plastic sleeves, with their anchorages placed in the prefabricated concrete elements.

3.2 3DPC structure: Load-bearing 3DPC V-columns and integrated floor slabs

The 3DPC structure of the tower consists in tripartite elements forming the load-bearing reinforced 3DPC V-columns: a concrete base, a 3DPC column and a concrete capital (Figure 2). The bases and capitals were prefabricated in concrete C40/50 and reinforced with mild steel.

They form part of the horizontal ring on each level (Figure 2), divided into eight units. In one ring, the capitals of the lower elements meet the bases of the upper elements with a usual offset of 22.5° , therefore overlapping each other and forming the floor slabs (Figure 3).



Figure 3. 3DPC structure assembly (level 3).

The 3DPC components are produced using the set-on-demand concrete extrusion process developed interdisciplinarily at ETH Zurich [12], [13], which allows rapid vertical build-up rates and precise control over the initial yield stress of the extruded concrete filament [14], [15].

The typical column branch cross-section is shown in Figure 4. Transverse reinforcement is integrated during the 3D-printing process using inter-layer $\varnothing 8$ stainless steel hoops. Initially, the hoops were placed manually as a proof of concept, but the process was later automated through a multi-robot fabrication system (Figure 5). The longitudinal reinforcement, 4-6 $\varnothing 16$ mm for each column branch, was introduced through hollow channels in the 3DPC elements and corresponding holes with finned sheeting tubes in the base and the capital. Because of the short anchorage length, the ends of the reinforcing bars were provided with threaded end anchors. After placing the bars, the holes were grouted. In case of post-tensioned elements, the high-

tension bars were also introduced and tensioned in this workshop. In addition, together with the transverse reinforcement ($\varnothing 8$ outer hoops spaced every 200 mm) installed during printing, inner loops ($\varnothing 8$ spaced every 400 mm), were included along the channels of the longitudinal reinforcement to prevent buckling [7] of the latter into the hollow columns.

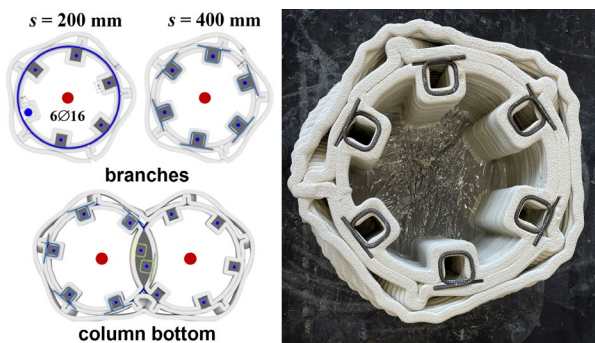


Figure 4. Typical column branch cross-section with hoops and inner loops, and installed inner loops during printing.



Figure 5. Robotic placement of transverse reinforcement.

4. Experimental campaigns

Between 2021 and 2024 experimental campaigns were carried out at ETH Zurich to assess the performance of load-bearing 3DPC and support the design of the Tor Alva columns. This included (i) a research of material characterisation including the strength of 3DPC by using the Modified Slant Shear Tests as well compressive tests on scaled-down 3DPC columns, and (ii) full-scale 3DPC V-column

tests. Details of (i) can be found elsewhere [2][7]. The focus of this section lies on the experimental results of the full-scale 3DPC V-column tests.

4.1 Full-scale 3DPC V-column tests

Load tests on full-scale reinforced 3DPC V-columns were carried out to validate the structural concept of the Tor Alva columns ensuring its required performance and structural integrity [7]. The specimens and the test setup represented the real 3DPC V-columns and their structural system of the third level of Tor Alva [15] (Figure 6), which is approximately 4 m high. As testing of full height columns was not feasible, half of those 3DPC V-columns were replicated and tested at full scale, preserving the structural behaviour of the whole V-columns. For testing, only the inner cross-section without the ornamental skin was considered. Figure 7 shows the structural system of an entire V-column and the equivalent system for a half-V-column.

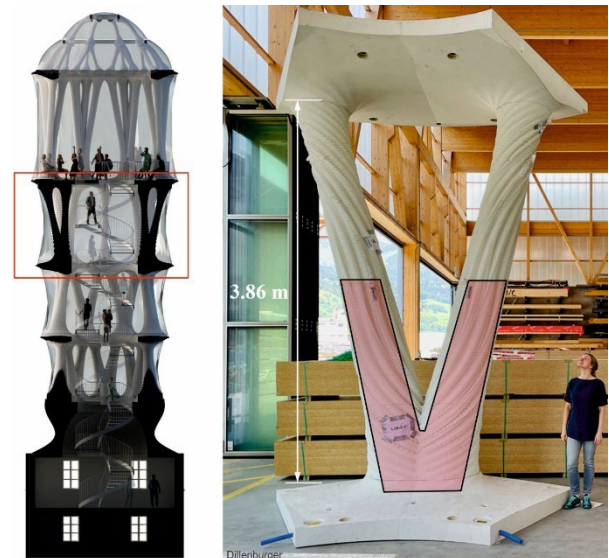


Figure 6. V-column of the third level of Tor Alva.

The structural response of the 3DPC V-column is highly efficient as the elements (branches and capital) work mainly in compression and tension when the V-column is subjected to both vertical and horizontal actions. Assuming similar rotational stiffness in the capital and base connections, the inflection point in the branches would be at mid-height (Figure 7b).

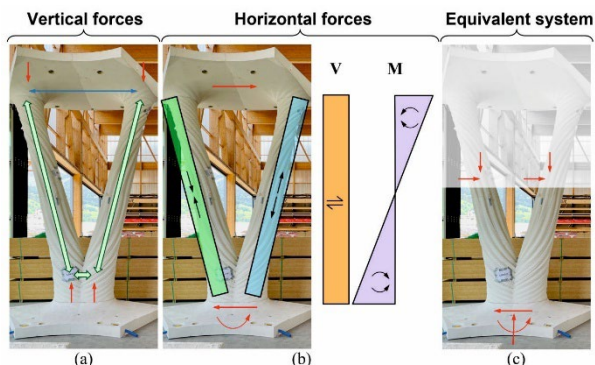


Figure 7. Structural system: a) Force system for applied vertical forces; b) Internal forces for applied horizontal forces; c) Equivalent structural system.

5.2.1. Specimens and test setup

The specimens (*S* and *SP*) were two full-scale reinforced 3DPC V-column halves of 2.1 m in height with integrated transverse and longitudinal reinforcement. Each specimen consisted in two branches inclined at approximately 14° from the vertical axis (Figure 8). The conical branches featured hollow cross-sections, intersected at the base, and included a construction joint connecting the lower and upper segments. Each branch was reinforced with six longitudinal bars $\text{Ø}16$ and transverse reinforcement $\text{Ø}8$ comprising hoops and inner loops spaced at 200 mm and 400 mm, respectively (Figure 8). The only distinction between the two specimens *S* and *SP* was the presence of an unbonded post-tensioned M20 rod in the core of each branch in Specimen *SP* (initial post-tensioning force of approx. 155 kN ($P_0 \approx 155$ kN)). Figure 8 illustrates the geometry of the specimens, the test setup and the cross sections.

The average compressive strength of the 3DPC was $f_{cm} = 55$ MPa (standard concrete test on cylinder specimens) estimating a compressive strength capacity in Section A-A (see Figure 8) of $N_{R,est} = 6.7$ MN. The specimens were tested to failure by applying similar vertical compressive forces, F_S and F_N (actuators of 1MN capacity), to the branches while simultaneously imposing a uniform horizontal displacement δ at their heads by a horizontal force H at approx. 2.0 m above the column bottom, as illustrated in Figure 8. The horizontal force H was applied only to the

southern branch whose horizontal head displacement opposed the imposed deformations induced by the vertical north force F_N . This load arrangement is referred to as *Load Case 1*.

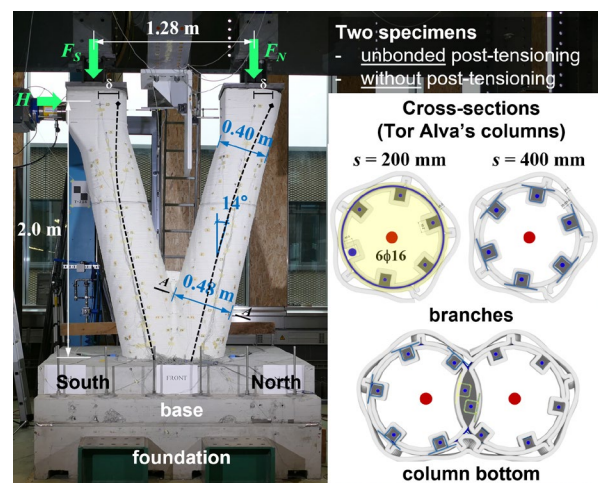


Figure 8. 3DPC specimens, test setup (*Load Case 1*) and cross-sections of Tor Alva's columns (level 3).

For *Load Case 1*, the test setup involved horizontal displacements at the heads of the specimens that were significantly larger than those expected for the Tor Alva V-columns at ULS. This approach was intentionally adopted as a conservative measure because it was anticipated that the 1 MN capacity of each actuator used to apply the vertical forces would be insufficient to load the specimens to failure if horizontal displacements were limited. Consequently, ductile failure was expected to occur under combined bending and compression.

Two additional load cases, *Load Case 2* and *Load Case 3*, were applied after ductile failure was achieved under *Load Case 1*. In *Load Case 2*, the south branch was subjected to a compressive force, while the north branch experienced a dominant tensile force. In *Load Case 3*, both branches were subjected to tensile forces.

The applied forces as well as the post-tensioning force on the specimens were monitored by load cells. The measurement system to continuously monitor the movements and rotations consisted of (i) LVDT's at the specimen heads (horizontal displacement), (ii) an NDI system (front face) with measuring stations

at the foundation, base of the column and along the specimen and (iii) inclinometers located on the specimen heads and base. In addition, specimen strains were manually measured by extensometers using stations spaced at 200 mm (front and back face), which were aligned with the most compressed and tensioned longitudinal reinforcement of the specimen branches.

5.3.1. Load-bearing capacity

Table 1 summarises, for the different load cases, the maximum forces applied to the specimens and their respective horizontal head movements.

The bearing capacity of the specimens under the different loading scenarios (load cases 1, 2 and 3) was significantly higher than the ULS design forces of the Tor Alva columns (level 3). Only for *Load Case 1* ductile failure was reached by applying compressive forces an order of magnitude higher than the design normal forces ($N_d < 0.05 \cdot N_{R,est}$) and imposing horizontal movements at the column heads δ that were considerably greater than those expected in the tower.

Table 1. Maximum experimental forces and horizontal displacements.

Load case	F_S F_N [kN]	H [kN]	δ_S δ_N [mm]	
<i>Specimen S</i>				
1	-277 -254	184	31.3 31.7	DF
1a	-325 -244	197	31.1 31.2	after DF
2	-464 256	228	31.2 -10.6	after DF
3	201 199	0	24.6 -10.7	after DF
<i>Specimen SP</i>				
1	-336 -301	196	18.0 36.9	DF
1a	-968 -260	277	-2.3 32.7	after DF
2	-510 294	223	4.9 -11.8	after DF
3	189 97	9	25.3 0.9	after DF

F_S and F_N : Vertical force in the south and north branches

H : Horizontal force in the south branch

δ_S and δ_N : Horizontal displacements at south and north branche heads

DF: Ductile failure by yielding of the reinforcement under dominant bending moment

For *Load Case 1*, a ductile failure in in the north column branch was caused by the dominant bending moment, with maximum horizontal movements of 32 mm and 37 mm for specimens *S* and *SP*, respectively. Figure 9 shows

the head displacements of the specimens as a function of shear forces and Figure 10 illustrates the maximum internal forces in the branches of Specimen *S* (without post-tensioning), taking into account the initial imperfections and 2nd order effects. Note that the axis of the actuators introducing the vertical forces underwent a rotation with respect to the vertical axis due to the horizontal displacement at the column heads, which generated an additional horizontal force ΔH .

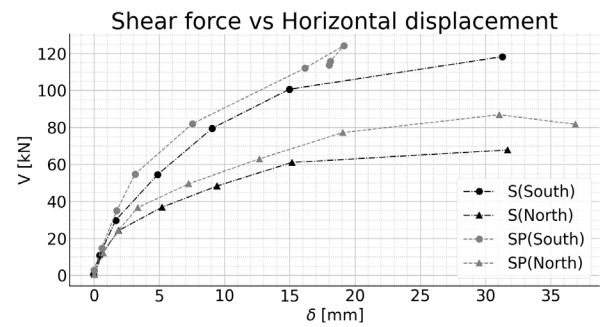


Figure 9. Shear force V – Horizontal movement δ diagram of the specimen branches.

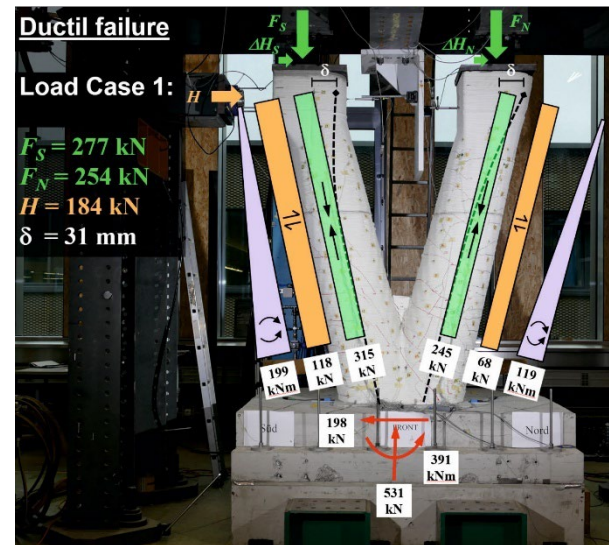


Figure 10. Ultimate forces, horizontal displacement and internal forces for *Load Case 1* in Specimen *S*.

The branches of the specimens were subjected to further extreme cases of dominant compression and tension (without reaching additional failure) by means of the other load cases. The maximum applied forces were limited by the test setup (actuator capacity and reaction frame) reaching a maximum vertical compressive force of 968 kN in the south branch

of Specimen *SP* (see *Load Case 1a* in Table 1, transition between *load cases* 1 and 2) and a maximum tensile force of 200 kN applied simultaneously in both branches of Specimen *S* (*Load Case 3* in Table 1).

5.3.1. Moment-curvature and crack pattern

The load-bearing V-columns exhibited a good performance both in ULS and for forces acting in the serviceability range, showing a similar behaviour to that expected in conventional RC elements. The north branches of the specimens exhibited a ductile failure, as shown in the moment-curvature diagram in Figure 11 corresponding to section A-A (see Figure 8).

The crack pattern was homogeneous with crack spacings s_r between 100 mm and 150 mm. Figure 12 shows the crack patterns of Specimen *S*. The cracks highlighted in red correspond to those generated after *Load Case 1* and those highlighted in black after *Load Case 3*, where each branch of the specimen was subjected to a vertical force of 200 kN (see Table 1). Interestingly, some cracks did not follow the layer joints, indicating that these joints were not as weak layers as often presumed.

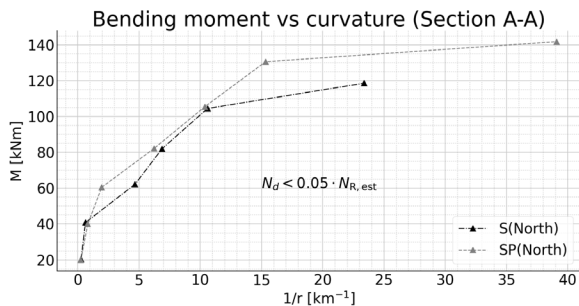


Figure 11. Bending moment – curvature diagrams of north column branches at Section A-A.



Figure 12. Crack pattern in Specimen *S*: after *Load Case 1* (red) and after *Load Case 3* (black).

5. Conclusions

The Tor Alva project and its associated research demonstrated the capabilities and advantages of DFC, enabling modular design, unique construction and large-scale structures with efficient assembly, while validating the use of reinforced 3DPC in fully load-bearing elements.

Although standard mortar and concrete tests provide valuable insight into the mechanical properties 3DPC, they fall short in addressing the material's non-isotropic behaviour due to the printed concrete layers [2], [7]. Full-scale load tests, especially in pioneering and innovative concepts, are essential to evaluate the influence of different parameters such as geometry, size effect, load introduction, construction joints, etc.

Full-scale structural projects are crucial for assessing DFC capabilities and verifying new concepts. However, experimental validation of each structure is excessively expensive and time consuming. A well-defined design basis for load-bearing 3DPC is thus essential to foster progress.

Reinforced 3DPC columns can provide powerful structural elements when combined with end pieces in conventional concrete. These end pieces facilitate the transition to other construction parts. Reinforcing 3DPC with hoops (acting as stirrups) and inner loops during the printing process has been refined at ETH. Combined with the principle of post-grouted longitudinal mild or post-tensioned bars yields monolithic structural elements whose behaviour can be reliably predicted.

The structural concepts of the load-bearing 3DPC columns including the reinforcement integration strategies were validated, exhibiting a good performance in terms of strength similar to that of conventional RC elements.

Acknowledgements

The authors would like to acknowledge the contributions of the Chair of Physical Chemistry of Building Materials at ETH Zurich, Zindel AG and Mesh AG. Research on load-bearing 3DPC

columns was funded by the Swiss Innovation Agency (Innosuisse), *3D Concrete Printing for Prefabricated Load-Bearing Columns* (project number 102.414.1 IP-ENG), and supported by the industry partners Zindel AG and Mesh AG. This work was funded by the Swiss National Science Foundation within the National Centre for Competence in Research in Digital Fabrication (project number 51NF40-141853).

References

- [1] F. P. Bos et al., ‘The realities of additively manufactured concrete structures in practice’, *Cem. Concr. Res.*, vol. 156, p. 106746, Jun. 2022 [Online]. Available: [10.1016/j.cemconres.2022.106746](https://doi.org/10.1016/j.cemconres.2022.106746).
- [2] L. Licciardello et al., ‘Determining the strength of 3D printed concrete with the Modified Slant Shear Test’, *Struct. Concr.*, 2025 [Online]. Available: [10.1002/suco.202400238](https://doi.org/10.1002/suco.202400238).
- [3] A. Anton et al., ‘Reinforcement lattices for 3DCP: A fabrication method based on ruled surfaces’, in *Structures and Architecture A Viable Urban Perspective?*, 1st ed., London: CRC Press, 2022, pp. 268–276 [Online]. Available: <https://www.taylorfrancis.com/books/9781003023555/chapters/10.1201/9781003023555-33> [Accessed: 29March2024].
- [4] L. Gebhard et al., ‘Inter-laboratory study on the influence of 3D concrete printing set-ups on the bond behaviour of various reinforcements’, *Cem. Concr. Compos.*, vol. 133, p. 104660, Oct. 2022 [Online]. Available: [10.1016/j.cemconcomp.2022.104660](https://doi.org/10.1016/j.cemconcomp.2022.104660).
- [5] L. Gebhard et al., ‘Experimental investigation of reinforcement strategies for concrete extrusion 3D printed beams’, in *13th fib International PhD Symposium in Civil Engineering*, 2020.
- [6] P. Bischof et al., ‘Experimental exploration of digitally fabricated connections for structural concrete’, *Eng. Struct.*, vol. 285, p. 115994, Jun. 2023 [Online]. Available: [10.1016/j.engstruct.2023.115994](https://doi.org/10.1016/j.engstruct.2023.115994).
- [7] A. G. Soto et al., ‘Structural Testing Campaign for a 30 m Tall 3D Printed Concrete Tower’, in *Fourth RILEM International Conference on Concrete and Digital Fabrication*, vol. 53, D. Lowke, N. Freund, D. Böhler, and F. Herding, Eds. Cham: Springer Nature Switzerland, 2024, pp. 493–500 [Online]. Available: https://link.springer.com/10.1007/978-3-031-70031-6_57 [Accessed: 13September2024].
- [8] M. van den Heever et al., ‘A mechanistic evaluation relating microstructural morphology to a modified Mohr-Griffith compression-shear constitutive model for 3D printed concrete’, *Constr. Build. Mater.*, vol. 325, p. 126743, Mar. 2022 [Online]. Available: [10.1016/j.conbuildmat.2022.126743](https://doi.org/10.1016/j.conbuildmat.2022.126743).
- [9] S. K. Kaliyavaradhan et al., ‘Test methods for 3D printable concrete’, *Autom. Constr.*, vol. 142, p. 104529, Oct. 2022 [Online]. Available: [10.1016/j.autcon.2022.104529](https://doi.org/10.1016/j.autcon.2022.104529).
- [10] B. Zareiyani and B. Khoshnevis, ‘Effects of interlocking on interlayer adhesion and strength of structures in 3D printing of concrete’, *Autom. Constr.*, vol. 83, pp. 212–221, Nov. 2017 [Online]. Available: [10.1016/j.autcon.2017.08.019](https://doi.org/10.1016/j.autcon.2017.08.019).
- [11] B. Panda et al., ‘Anisotropic mechanical performance of 3D printed fiber reinforced sustainable construction material’, *Mater. Lett.*, vol. 209, pp. 146–149, Dec. 2017 [Online]. Available: [10.1016/j.matlet.2017.07.123](https://doi.org/10.1016/j.matlet.2017.07.123).
- [12] L. Reiter et al., ‘Setting on demand for digital concrete – Principles, measurements, chemistry, validation’, *Cem. Concr. Res.*, vol. 132, p. 106047, Jun. 2020 [Online]. Available: [10.1016/j.cemconres.2020.106047](https://doi.org/10.1016/j.cemconres.2020.106047).
- [13] A. Anton et al., ‘A 3D concrete printing prefabrication platform for bespoke columns’, *Autom. Constr.*, vol. 122, p. 103467, Feb. 2021 [Online]. Available: [10.1016/j.autcon.2020.103467](https://doi.org/10.1016/j.autcon.2020.103467).
- [14] A.-M. Anton et al., ‘Column-Slab Interfaces for 3D Concrete Printing: Design, Fabrication and Assembly Strategies’, 2022 [Online]. Available: <http://hdl.handle.net/20.500.11850/639150> [Accessed: 7January2025].
- [15] A. Anton et al., *Tor Alva: A 3D Concrete Printed Tower*. Fabricate 2024, UCL Press 2024, 2023.